Properties of Silver Clusters Adsorbed to Silver Bromide

R. C. Baetzold

Imaging Materials and Media, R&D, Eastman Kodak Company, Rochester, New York 14650-2021

Received: October 19, 2000; In Final Form: January 8, 2001

Density functional calculations of the structure and electronic properties of silver clusters interacting with a fragment of silver bromide that is embedded within a polarizable representation of the AgBr crystal are presented. Flat (001) surfaces and kinked surfaces are considered. The optimized geometry of the silver clusters is nearly planar for the clusters up to four atoms that are considered. We examined the degree to which different surface defect sites could modulate the properties of the adsorbed silver cluster. The positive kink site is unique in providing a location where the neutral cluster can capture photoelectrons. This effect can be rationalized by electrostatic arguments and is consistent with this site functioning as a location for photolytic silver formation. Other kink sites of neutral or partial negative charge do not permit electron trapping at neutral silver clusters. These sites could act as locations for chemically produced silver clusters. Calculations are presented showing that some geometries of Ag_3^+ adsorbed at the negative kink can trap electrons in accord with a proposal by Tani. The calculations are used to compare different mechanisms for photolytic formation of silver clusters. They can be compared to gas-phase calculations adjusted for the interaction with a polarizable surface to show that both calculations agree that cationic silver clusters are unstable with respect to dissociation except on the negative kink. The calculations show a deep electron trap depth for the silver atom consistent with its participation in the nucleation phase of silver cluster growth during photolysis. A sulfide ion substituted for bromide at a positive kink is shown to provide a means of coupling the electron to the crystal ions.

I. Introduction

Several aspects of the formation of small silver clusters by photolysis of silver bromide have been well-established within a photographic context. It is broadly accepted that interstitial silver ions react with trapped photoelectrons to build silver clusters. Measurements of the temperature dependence of electron lifetime and field decay have established[1] that the electron is first trapped at a site on the surface followed by motion of the interstitial silver ion to the electron. The further enlargement of silver clusters can be understood to occur through transport of the mobile photoelectrons and interstitial silver ions and accumulation at one or at most a few growing centers. ESR experiments[2] have also shown evidence for electron trapping in effective mass states that were extended lattice dislocations that penetrated the surface. Microwave photoconductivity experiments[3] showed rapid electron trapping at sites thought to be surface kinks on a time scale of 10 ns at room temperature. This initial trapping was followed by a temperature-activated process thought to involve rearrangement of the surface kink induced by the trapped electron and preceding the formation of a silver atom. These and other mechanisms involving surface kinks and shallow−deep transitions are discussed in a recent review.[4] Sensitizing agents such as sulfide are known to play an important role in controlling the site of and the efficiency of silver cluster formation.[5] When the silver cluster reaches a critical size,[6] it becomes possible to catalyze the chemical reduction of the silver halide grain in the presence of certain solution reducing agents. Many other points in the mechanism are established,[5] but a major limiting factor to complete detailed understanding is the complexity of the photographic system. Much of the understanding is deduced from experimental measurements on macroscopic systems, while many microscopic details even today cannot be measured directly. Thus, there are continued attempts to better understand the steps in the mechanism of photolysis of AgBr.

Computations[7] have been utilized to study a variety of phenomena involved in silver halide photolysis. These have employed a small cluster treated by density functional methods and embedded within a polarizable medium that represents the long-range effects of the ionic silver halide crystal. Several trends were apparent in these calculations including the importance of surface defect sites in determining electronic properties of the adsorbed silver cluster. As a first approximation, this result may be understood on the basis of the Madelung field that is modulated by the local structure of the defect site. Thus, near defect sites containing an accumulation of positive or negative ions the local Madelung potential is shifted and this stabilizes or destabilizes the electrons of an adsorbate, respectively. This effect is observed despite the presence of the partial covalent bonding character of the silver halide that is treated quantum mechanically. Interestingly, the effect of local surface structure had been found in earlier semiempirical calculations[8] and was used to interpret the behavior of photolytic versus chemically formed silver clusters. We extend the earlier work through the investigation of various sized silver clusters at different orientations near particular defect sites by the application of larger embedded quantum models.

In addition to the improved calculations reported here, we wish to examine some general questions that have been discussed from an experimental standpoint in the recent literature. One area of contemporary interest involves the study of chemically deposited silver clusters and how their properties compare to photolytically formed clusters. We will examine

10.1021/jp003860a CCC: $20.00
Published on Web 04/11/2001

various concepts proposed for these centers. There are also different views of some steps in the fundamental mechanism of photolytic silver formation from silver bromide. The most widely accepted model is based upon the work of Gurney and Mott[9] and is a synthesis of experimental and theoretical results referred to as the nucleation and growth model.[10] The model has been quantitatively developed by the use of Monte Carlo calculations, and a recent version of the calculation has been described.[11] The model holds that alternating electronic and ionic steps are needed to ensure the growth of silver clusters from the single atom stage. Some of the steps in this mechanism have been questioned by Mitchell,[12] who has presented some alternatives. Experiments have been brought to bear on the resulting questions, but in this work we will only approach the questions from a computational viewpoint.

We first consider some of the issues compared in the different mechanisms of photolysis that can be studied by computations. One question concerns the role of the single silver atom and whether it possesses properties that would allow it to grow to become a larger silver cluster. The nucleation and growth mechanism holds that this unstable center forms and decays many times until eventually one silver atom attracts a photoelectron during its lifetime and forms the silver anion that can capture a mobile interstitial silver ion leading to the stable silver dimer. Experiments[13] of variable light intensity are cited to support this step. In the alternative mechanism[12] it is considered that the unstable silver atom forms but decomposes, representing a wasted loss process from the point of view of efficient formation of a silver center in high-speed systems. In this latter model it is proposed that silver dimers are formed during preparation of the silver halide grain and these provide a precursor center for growth to larger silver clusters through attraction of silver ions and photoelectrons. These different views thus also relate to the issue of the degree to which chemically and photolytically formed clusters differ and whether chemically formed clusters can act as a precenter for growth of silver clusters.

A second major point of discussion is whether the growing small silver cluster passes through a cationic state, Ag_n^+. In the proposal by Mitchell[12] this center is proposed to first form for Ag_4^+ followed by electron trapping. In the nucleation and growth mechanism, the neutral silver cluster is presumed to be able to attract and trap a photoelectron followed by an interstitial silver ion. The distinction between the two proposals may seem rather small from the point of view that the end result of either sequence is the same and that mobile interstitial silver ions are present in AgBr that might be adsorbed to convert a neutral silver cluster to the cation or convert an anion silver cluster to neutral. On the other hand, from an electrostatic point of view the distinction is rather important since the ability to trap photoelectrons should be quite different at a neutral or cationic silver cluster. This factor, in turn, will be important in influencing the reactivity of silver centers with charged reagents. The positions of the energy levels of the cluster relative to the conduction band edges will control whether clusters of a given charge can trap electrons. This broad question even encompasses the first point discussed above since a neutral silver atom must be able to capture a photoelectron for the nucleation and growth mechanism to operate.

A final point of difference in the two mechanisms that we will consider involves the role of sulfur sensitizers. In one model, molecules of Ag_2S are thought to capture a photohole that forms a center like Ag_2S^+ that, in turn, decomposes releasing an interstitial silver ion leaving the AgS molecule and creating an electron. In the nucleation and growth model, the center containing molecules of Ag_2S functions as electron traps that provide a site for the growth of the photolytic silver cluster.

Chemically deposited silver clusters have been studied for photographic effects. It has long been stated that the properties of chemically formed and photolytically formed silver clusters differ.[14] Proposals have been presented to explain these differences.[15−20] Original studies showed that chemically deposited silver clusters do not attract electrons or grow to form larger silver clusters. Recent work[21,22] has shown evidence that a chemically formed silver cluster in some conditions can act as an electron trap. Tani[23−25] has proposed this center to be comprised of Ag_3^+ located at a surface negative kink. From a charge standpoint this center is equivalent to Ag_2 located at a positive kink since it is well-known that a silver ion can adsorb and convert a negative kink to a positive kink. At the same time the Ag_2 center at a positive kink is believed to form photolytically[8] and is termed a P center. One might consider whether the two centers mentioned here will possess the same physical properties or if they differ in some ways. The physical properties of the chemically deposited silver clusters have been extensively studied[26,27] and evidence presented that they consist of Ag_2.

This work represents an extension of previous studies[7b] of silver clusters using an embedded cluster model. In particular, the quantum cluster has been enlarged and the treatment of its interactions with the surrounding crystal ions made more complete. The purpose of this work is to present a detailed study of silver clusters adsorbed to a cubic AgBr surface containing various defect sites so that we may examine various steps in the mechanism of AgBr photolysis leading to silver clusters. We employ a large embedded cluster model within the density functional framework that is discussed in Methods. In Results we present the intrinsic calculated properties of silver clusters including the structure, binding energy, ionization potential, and electron affinity. We also investigate the effects of sulfur near a positive kink site. Then we turn to the mechanism of silver cluster formation and how our results bear upon particular steps of the reaction. In Discussion we explore how these results compare with other calculations and experiment.

II. Method

The embedded cluster method was used to represent silver clusters of varying size adsorbed to different sites on a AgBr surface. The calculation proceeds in two stages. The first stage is a quantum mechanical calculation of a cluster of Ag_n adsorbed to the appropriate cluster of AgBr. This entire quantum mechanical unit was embedded in an array of approximately 3000 point charges representing silver and bromide ions. The point-charge array contained unit charges and is chosen to give an overall zero charge cluster and point ion array representing the AgBr surface. For the planar (001) surface, an Ag_9Br_8 quantum cluster replaced the appropriate point-ions in the center of the flat surface of the hemisphere. For the kink models, quantum units such as $Ag_{11}Br_{10}$ were attached to the flat hemispherical surface and additional point ions added as necessary to complete missing parts of the top layer of the model. The quantum mechanical units representing positive kinks (+K) and positive double kinks (+DK) are shown in Figure 1. The comparable negative kink (−K) and negative double kink (−DK) are obtained by interchanging anions and cations in both the quantum mechanical and point-ion arrays. An additional feature of the model involves replacing positive point ions adjacent to the quantum mechanical model by full-

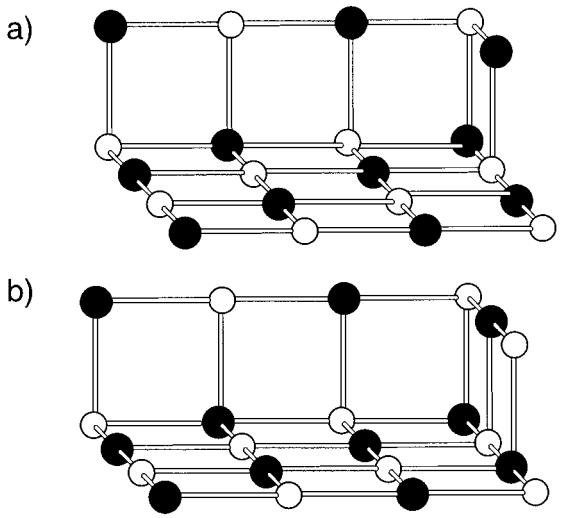

Figure 1. Structure of the quantum mechanical units $Ag_{11}Br_{10}$ representing the positive kink in a and $Ag_{11}Br_{11}$ representing the positive double kink in b. These quantum clusters are embedded in the point ion arrays also containing full pseudopotentials described in the text. Open circles are Br^-, and filled circles are Ag^+.

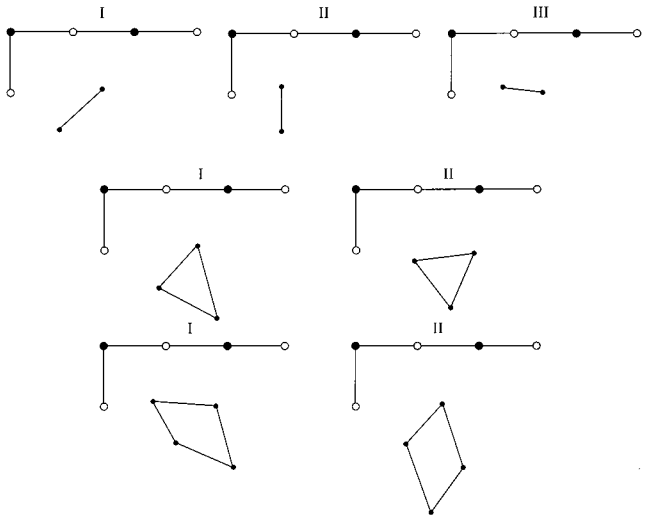

Figure 2. Drawing showing the most stable structures found for Ag_2, Ag_3, and Ag_4 near the positive kink in the quantum mechanical part of the calculation. A top view is shown with just the top plane of Ag^+ and Br^- quantum ions.

core pseudopotentials[28] representing Ag^+ in order to reduce possible unphysical effects of artificial polarization of anions adjacent to the point ions. Thus, the overall quantum mechanical units treated were as follows: $Ag_{11}Br_{10}Ag_{19}$ for +K, $Ag_{11}Br_{11}$-Ag_{20} for +DK, $Ag_9Br_8Ag_8$ for flat, $Ag_{11}Br_{11}Ag_{20}$ for −DK, and $Ag_{10}Br_{11}Ag_{19}$ for −K. The latter subscripted silver ions denote the full pseudopotential ions and will not be designated further. These kink models for sites of photolytic silver cluster formation are similar to those we first introduced[8] in semiempirical calculations. The double kinks and flat surface are expected to possess an effective zero charge while the single kinks are commonly assumed to possess an effective long-range half-charge with the sign depending upon the type of kink.

The first stage of the calculation proceeds by fixing the position of the AgBr quantum cluster ions, full core pseudopotential[28] ions, and the point charges. The B3LYP functional[29] is employed with the Gaussian 98 code[30] to determine the electronic properties of the quantum mechanical unit. The geometry of the neutral silver cluster is optimized in order to find an equilibrium structure. The criterion for convergence is taken as the default of the program. In some cases when convergence did not occur after 60 cycles of optimization, we continued until achieving an energy difference of 0.000 05 au between successive cycles of SCF. The initial starting geometries were chosen similar to successive smaller sized clusters, although other starting structures were often considered. The most stable geometries for the neutral silver clusters are shown for clusters near the positive kink site in Figure 2. We often find local energy minima structures such as those shown in Figure 2 for the Ag_2, Ag_3, and Ag_4 center. The anion and cation geometries were also optimized and found to have only small displacements from the neutral structures.

In the second stage of the calculation the polarization energy component due to the relaxation of surrounding ions in the AgBr unit was calculated. This determines a polarization energy that is added to the quantum mechanical energy. The procedure has been described before.[7b] It involves representing the lattice ions within the shell model in a surface calculation[31] that employs pairwise short-range potentials and Coulomb interactions. The potential was that of Catlow et al.[32] determined by fitting to the dielectric, elastic, and point defect properties of bulk AgBr. A separate calculation is applied for each charge state of the silver cluster. The total energy differences of appropriate charge states were used to calculate the ionization potential (IP) and electron affinity (EA). Typical displacements of AgBr ions are indicated in the Appendix.

We should be aware of some of the parameters and approximations in this calculation. The polarization calculation is accomplished in a second calculation following the quantum mechanical calculation, so the overall procedure is not fully self-consistent. We plan to investigate this approximation in the future by a fully self-consistent procedure[33,34] in order to allow the silver cluster and surrounding AgBr ion positions to be optimized simultaneously. We employed LANL2DZ basis functions and the corresponding small-core pseudopotentials[35] for Ag and Br ions. Polarization functions were not employed since our studies on silver clusters using density functional methods showed their effect to be small and excluding them made it possible to enlarge the quantum mechanical cluster. We employed the largest clusters possible permitting calculations to be completed in reasonable times. Small core pseudopotentials on Ag and Br were used because it is known that significant hybridization of Ag 4d and Br 4p orbitals takes place in the valence band of AgBr.[36]

We tested the B3LYP functional with LANL2DZ basis functions for bare silver clusters as a check of the method. The calculation was performed with and without f polarization functions.[37] The cluster geometry was optimized and the vertical ionization potential and electron affinity were calculated. We found an isosceles triangle for Ag_3 and a rhombus for Ag_4 as the most stable geometry. The results are shown in Table 1 where it can be seen that the f polarization functions did not have a major effect on the IP and EA results. These values carry a typical error of 0.2−0.4 eV compared to experiment. For $n = 1-3$, the calculated IP is too large and the calculated EA is too small. For $n = 4$, the calculated IP and EA are too small compared to experiment. The errors in these values could possibly be used to correct the calculated IP and EA values of adsorbed silver clusters, although we have not taken this tact in this work.

III. Results

Geometry of Adsorbed Silver Clusters. The geometry of small silver clusters adsorbed near a defect site on the AgBr

TABLE 1: Calculated Vertical IP and EA of Silver Clusters[a]

	no *f* function ions		*f* function ions		expt[b−d]	
size	IP	EA	IP	EA	IP	EA
1	7.75	1.09	7.75	1.09	7.57	1.30
2	7.80	0.93	7.81	0.92	7.56	1.06
3	6.85	2.13	6.85	2.22	6.20	2.43
4	6.43	1.54	6.44	1.54	6.65	1.65

[a] Properties at calculated equilibrium geometry, isosceles triangle for $n = 3$ and rhombus for $n = 4$. [b] Jackschath, C.; Rabin, I.; Schulze, W. *Z. Phys.* **1992,** *D22,* 517. [c] Almeddin, G.; Hunter, J.; Cameron, D.; Kappes, M. M. *Chem. Phys. Lett.* **1992,** *192,* 122. [d] Ho, J.; Ervin, K. M.; Lineberger, W. C. *J.* Chem. Phys. **1990,** *93,* 6987.

TABLE 2: Properties Calculated for Silver Clusters near the Positive Kink Site

cluster size	orientation	BE (eV)	IP (eV)	EA (eV)
2	I	2.78	7.00	3.87
	II	3.04	7.49	3.81
	III	2.88	7.17	4.10
3	I	3.63	5.88	4.03
	II	3.72	5.96	4.22
4	I	5.52	6.26	3.97
	II	5.07	6.20	4.07

surface is determined through an optimization procedure. The appropriate atoms or ions are placed in an initial configuration near the defect, and a final equilibrium structure is determined by displacing the cluster atoms or ions according to the forces it experiences until the lowest energy is obtained. We have found that there are local energy minima for dimers and larger clusters depending upon the initial configuration selected and will illustrate these results for the positive kink defect site in the quantum mechanical part of the calculation. The single silver atom occupies a position very near the virtual defect site for the addition of the next ion to the model. Three structures for the dimer are close in energy. These are sketched in Figure 2 where the orientation near the ions of the positive kink is shown and the appropriate properties are given in Table 2. The structures differ mainly by the orientation of the silver−silver bond axis. According to the total binding energy in Table 2, structure II is most stable, but the energy differences between different orientations are very small. The distances to the closest crystal silver ions are 3.17 and 2.81 Å for one atom and 4.59 and 2.72 Å for the second atom in structure II. The Ag−Ag bond length is 2.64 Å. Two configurations for the trimer are found that are very close in energy. In each case the neutral cluster takes a triangular shape with different orientations with respect to the positive kink. The Ag−Ag distances in the most stable cluster (II) are 2.70, 2.85, and 2.76 Å. The tetramer takes the shape of a trapezoid, and two orientations are shown in Figure 2. The most stable structure (I) has Ag−Ag distances of 2.97, 2.80, 2.75, and 3.27 Å. The coordinates of the most stable structures for Ag_n, $n = 1-4$, are given in Table 3. These structures are closest to planar in shape. In the case of the Ag_4 cluster we also investigated a three-dimensional pyramid shape as a starting configuration and found that the structure relaxed to a nearly planar structure indicating its lack of stability. In addition to the binding energies, the electron affinity and ionization potentials are shown in Table 2. There are only small differences in these values for the different orientations.

We studied several clusters at the double kink, planar, and negative kink models. At the kink sites, the most stable structures were similar to the structures found at the positive kink with small differences in bond lengths. The most stable structures calculated in the quantum mechanical part of the

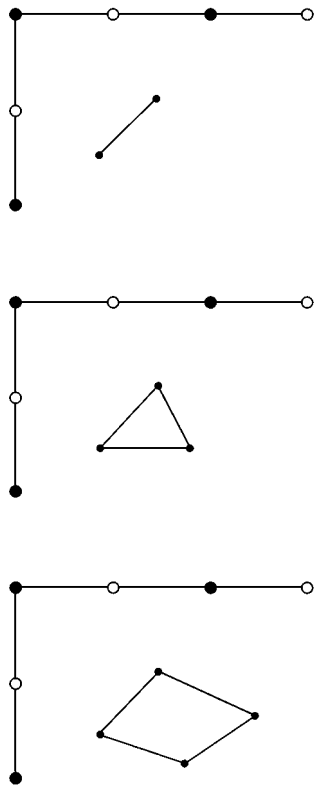

Figure 3. Drawing showing the calculated structures for Ag_2, Ag_3, and Ag_4 near the positive double kink in the quantum mechanical part of the calculation. A top view is shown with just the top plane of Ag^+ and Br^- quantum ions.

TABLE 3: Positions of Silver Atoms near Positive Kink Relative to Virtual Site

cluster	*X* (au)	*Y* (au)	*Z* (au)
Ag	0.1050	0.1915	0.2312
Ag_2	1.2946	0.7215	2.9649
	1.4710	2.8081	0.5657
Ag_3	0.7291	0.5058	1.4601
	4.4228	0.2817	0.5103
	2.5213	4.4080	0.1842
Ag_4	1.3283	0.9070	2.8586
	3.9526	0.4881	1.0213
	0.3828	3.0840	0.1678
	5.4691	5.4759	0.4470

calculation for $n = 2, 3, 4$ at the +DK are shown in Figure 3. The shape of the cluster is also nearly planar in these cases. The flat (001) surface model has a silver ion in the center of the surface model. On this surface, the first silver atom adsorbs over a hollow site having nearest neighbors of two silver ions and two bromide ions. The dimer is most stable with bond midpoint over the central silver ion. The trimer has the general shape of an obtuse triangle, and the tetramer has a silver atom added to the end of the trimer structure.

Binding Energy of Adsorbed Silver Clusters. The binding energies of neutral, cationic, and anionic clusters were calculated at each defect site on the AgBr surface. These values represent the binding energy with respect to the separated cluster model and separated ions or atoms of the adsorbed silver cluster. The charged states also include a polarization energy contribution calculated as described earlier. The results for the most stable neutral clusters are shown in Table 4. The binding energies vary strongly with the site of adsorption. For example, the adsorption energy of a neutral silver atom is greatest at the positive kink and smallest at the flat surface. This behavior is consistent with strongest bonding to sites exposing atoms of lowest coordination

TABLE 4: Calculated Binding Energies (eV) versus Isolated Model and Ions or Atoms

cluster size	neutral	cation	anion
	$Ag_{11}Br_{10}$, +K		
1	0.88	1.38	4.71
2	3.04	3.30	5.76
3	3.72	5.51	6.85
4	5.52	7.01	8.37
	$Ag_{11}Br_{11}$, +DK		
1	0.76	2.29	2.86
2	2.71	5.21	4.23
3	3.65	6.45	4.85
4	4.99	7.21	6.45
	Ag_9Br_8, Flat		
1	0.22	2.49	2.63
2	1.92	3.72	3.77
3	2.62	4.45	4.91
4	4.02	6.03	5.46
	$Ag_{11}Br_{11}$, −DK		
1	0.54	2.96	1.95
2	1.88	4.35	4.46
3	3.57	6.60	5.91
4	5.20	8.14	7.38
	$Ag_{10}Br_{11}$, −K		
1	0.33	4.72	1.20
2	1.87	5.36	2.69

and would be expected on the basis of theories of active surface sites. The cationic clusters have the strongest binding energy at the negative kink, and the anionic clusters have the strongest binding at the positive kink. In each case, the more neutral double kinks and flat surface have intermediate values. This trend reflects the fact that the single kink sites behave as if they possess an effective charge and that the resulting Coulombic effects play an important role in determining the overall binding energy of the charged clusters. Note that since each AgBr cluster model has a net zero charge, the effect we report is due to the local defect structure of the single kink sites.

The binding energies of the silver cluster increase with its size of the cluster. At each defect site the cluster is stable with respect to dissociation into single silver atoms

$$Ag_n \rightarrow nAg \tag{1}$$

indicating a driving force toward aggregation from the separated adsorbed atoms. We consider the separated atoms at the same defect site as the silver cluster in making this comparison. The strongest binding of cationic clusters is at the negative kink. However, in view of the fact that adsorption of a silver ion converts a negative kink (−K) to a positive kink (+K),

$$(-K) + Ag^+ \rightarrow (+K) \tag{2}$$

binding of a cationic cluster to a negative kink might be considered analogous to the binding of the next smaller neutral cluster to the positive kink. While this effect is true on a large scale, our calculations give small deviations from the principle because of slightly different adsorption geometries for neutral and charged clusters. For example, we can consider the adsorption energy of Ag_2^+ at a negative kink compared to Ag at a positive kink. Subtracting the Ag^+ adsorption energy to the negative kink from the Ag_2^+ binding energy gives 0.64 eV compared to 0.88 eV for the Ag binding energy to the positive kink using the data in Table 4. Other comparisons could be made, but they reflect small differences due to different equilibrium positions of the charged and neutral clusters.

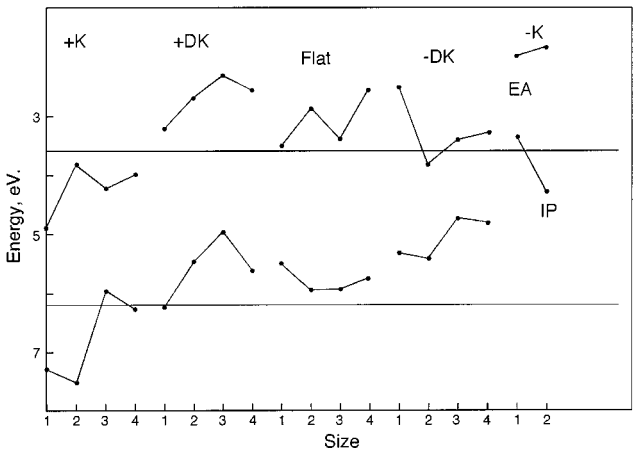

Figure 4. Plot of calculated IP (lower curves) and EA (upper curves) for small silver clusters adsorbed near different defect sites on the AgBr surface.

TABLE 5: Calculated Ionization Potential and Electron Affinity of Silver Clusters Adsorbed to Various AgBr Models

cluster size	+K	+DK	flat	−DK	−K
	Ionization Potential (eV)				
1	7.25	6.22	5.48	5.33	3.36
2	7.49	5.47	5.95	5.39	4.27
3	5.96	4.95	5.92	4.73	
4	6.26	5.60	5.75	4.82	
	Electron Affinity (eV)				
1	4.92	3.19	3.49	2.50	1.95
2	3.81	2.67	2.85	3.81	1.82
3	4.22	2.29	3.37	3.42	
4	3.97	2.55	2.53	3.27	

We can compare the binding energy of two Ag_2 molecules to one Ag_4 molecule. At each kink site, the two dimers are more stable than the tetramer. On the flat surface the tetramer is slightly more stable, although the flat surface is a rather unfavorable site for binding silver clusters compared to the single or double kink sites. The flat surface gives a small value for the binding energy of the single silver atom compared to the kink sites. The strong binding of a silver atom at the positive kink shows that this is a preferred site for the formation of silver atoms during photolysis. This large value contributes significantly to the initial formation of silver atoms during photolysis. The large clusters become stabilized even more as their binding energy per atom approaches the bulk cohesive energy. The largest value for a Ag_4 cluster in Table 4 only approaches about half of the bulk cohesive energy.

Ionization Potential and Electron Affinity of Adsorbed Silver Clusters. The ionization potential (IP) and electron affinity (EA) are determined by the difference in total energy of the appropriate thermally relaxed charge states. The reference levels for the silver bromide crystal that we have used previously for this thermal IP and EA are 3.6 eV for the conduction band edge and 6.2 eV for the valence band edge. The calculated values of the IP and EA are given in Table 5 for each defect site and are plotted in Figure 4. These values reflect the Coulombic effects due to partial charges associated with single kink sites such that the IP and EA values at a given cluster size fall in the order (+K) > flat > (−K) with intermediate values for the DK sites. Consider the IP values that are largest at the positive kink. At this site, Ag and Ag_2 would not be expected to react with a photohole at the valence band edge (6.2 eV). This behavior is practically unlike that for all silver clusters at other defect sites where IP < 6.2 eV permitting reaction of the

photohole with the cluster. We have also observed this behavior in earlier semiempirical[8] and ab initio calculations[7b] and interpret this as a reason for the stability of photolytic Ag_2 formed at a positive kink versus instability of chemically formed Ag_2 at flat or double kink sites. These latter sites are present in much greater concentration than positive kink sites, so they may function as sites for silver clusters formed in chemical reduction. Many experiments[14,15] have shown that in the presence of photoholes, chemically formed Ag_2 centers are oxidized. Our calculations shown in Table 5 also indicate that if larger clusters such as Ag_3 or Ag_4 were formed at the double kink or flat sites, they would also react with holes.

The EA values determine whether a photoelectron in the conduction band can be trapped at the neutral silver cluster. This electron trapping requires that EA > 3.6 eV It is clear that this reaction is possible at the sequence of clusters Ag_n ($n = 1-4$) located only at the positive kink. This clear distinction with the other surface sites is an indication of special activity at the positive kink site where the photolytically formed neutral clusters can trap photoelectrons.

Ag Atom Pathways. We turn to the question of whether Ag atoms represent a wasted step or a necessary step in the formation of photolytic silver clusters. Consider whether the unstable silver atom can trap a photoelectron. The data in Table 5 show that this is possible only when the atom is located at the positive kink where it has a trap depth of approximately 1.3 eV. Thus, there is favorable thermodynamics for electron trapping at this atom stage. The lifetime of the photolytic silver atom is deduced from experiment[13] to be of the order of 1 s or less. During such a time scale a photelectron can diffuse distances much greater than the dimensions of the silver halide grain based upon its reported mobility.[38] Thus, during the Ag atom lifetime, there is the opportunity for a photoelectron to be trapped to form Ag^- anion. Of course, the trapping process may not proceed with unit efficiency because of the 1.3 eV trap depth that requires efficient loss of energy of the electron by transfer to the lattice. This subject is more fully discussed by Hamilton[39] in a paper dealing with the strong coupling to the lattice.

Consider the process responsible for the instability of the silver atom. It is thought to be the microscopic reverse of its formation[10] and proceeds as

$$Ag \rightarrow Ag^+_i + e^- \qquad (3)$$

where Ag^+_i, the interstitial silver ion, is first ejected followed by loss of the trapped electron to the conduction band. The energetics of this reaction can be calculated from a Born−Harber cycle as

$$\Delta E = E(Ag) + 7.56 - 3.6 - E(Ag^+_i) \qquad (4)$$

where the total energy change in electronvolts requires the binding energy of the silver atom (E(Ag)) at a particular site and the interstitial silver ion ($E(Ag^+_i)$). The latter is difficult to calculate directly with the embedded cluster models of the type we study here. Experiment[40] shows that the energy to form an interstitial silver ion by release from a positive kink is several tenths of an electronvolt. This value should be subtracted from the value of the Ag^+ binding energy at the negative kink (4.72 eV) to obtain $E(Ag^+_i)$. Unfortunately, the formation energy value is not known well, but a separate study using the shell-model potential in a surface calculation[41] gives 4.31 eV as the value for $E(Ag^+_i)$. This value is consistent with expectations discussed above. Using the data in Table 4, we find the following energies for reaction 3: 0.53 eV at +K, 0.41 eV at +DK, −0.13 eV at flat, 0.19 eV at −DK, and −0.02 eV at −K. These values show that the silver atom is most stable at the positive kink, where it is weakly stable. Thermal fluctuations could lead to its decay. We attach more significance to the trends in these data than their absolute values because of the approximations in this estimation.

TABLE 6: Calculated Energy of Reaction (eV) for $Ag_n + Ag^+_i \rightarrow Ag_{n+1}^+$

n	+K	+DK	flat	−DK	−K
2	1.89	0.14	0.81	0.50	0.72
3	1.84	0.57	1.78	0.14	
4	1.02	0.75	0.90	0.26	

Binding of Silver Ions to Neutral Clusters. We compute the binding energy of silver ions to neutral silver clusters. Using the interstitial silver ion reference state, we can write

$$Ag_n + Ag^+_i \rightarrow Ag^+_{n+1} \qquad (5)$$

where the neutral and cationic cluster are located at the same surface site. Using the binding energy data in Table 4, we can calculate the energy required for reaction 5, as given in Table 6. We observe that this reaction is always endothermic for the sites such as +K, flat, and usually +DK. In the case of the −K site, the reaction is exothermic. There is no driving force for attracting silver ions to the neutral silver clusters on most surface sites, including the positive kink where latent image formation occurs photolytically.

Chemically Formed Silver Centers. There has been much work involving chemically formed silver centers on the surface of silver halide. There is considerable agreement that some of the chemically formed centers can trap photoholes. An early proposal by Tani[19,20] suggested that these clusters were formed at neutraly charged sites, and we have performed several calculations[7,8] indicating that Ag_2 at a double kink site could perform this function. These were termed R centers. Physical studies of chemically deposited silver centers have also indicated that some centers have the ability to trap electrons. A question comes up regarding how these later centers compare with photolytically formed silver centers such as Ag_2 that also can trap electrons. Indeed, our earlier calculations and the results reported here indicate that Ag_2 at a positive kink can trap electrons and are termed P centers. In his work, Tani[21−23] has also termed the electron trapping reduction centers P centers and assigned a structure of Ag_3^+ at a negative kink. It is recognized that because of the different modes of formation of photolytic and reduction centers that the two types of P centers may have some different properties. We study this question in order to make comparisons of the properties of different centers.

We have compared the properties of Ag_3^+ at a negative kink with Ag_2 at a positive kink. Of course, from a purely electrostatic point of view the two centers are equivalent because of the conversion of a negative kink to a positive kink through the adsorption of a silver ion as in eq 2. However, structurally the two centers may be different depending upon when the silver ion is incorporated into the forming Ag_3^+ center. If the silver ion is first added to the negative kink prior to addition of Ag_2, the equilibrium structures of the final clusters should be the same. However, if Ag_2 is first formed at a negative kink before the silver ion is added, the two centers could have a different structure that may remain distinct depending upon the energy barriers for rearrangement. Moreover, there is the possibility of local energy minima near some sites that could contribute to such activation barriers and thus lead to a range of different properties.

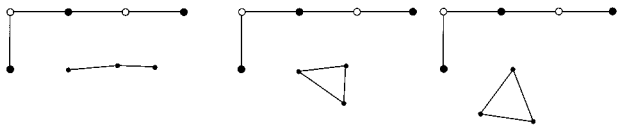

Figure 5. Structure of three calculated geometries for Ag_3^+ adsorbed near the negative kink in the quantum mechanical part of the calculation.

TABLE 7: Calculated Properties of Ag_3^+ Centers on AgBr[a]

cluster	kink site	structure	EA (eV)	IP (eV)	BE (eV)
Ag_3^+	-K	linear	3.30	7.22	7.44
Ag_3^+	-K	triangular, I	3.41	7.12	7.48
Ag_3^+	-K	triangular, I I	3.64	7.48	7.64

[a] BE = binding energy of Ag_3^+ at −K.

We applied the embedded cluster method to treat Ag_3^+ adsorbed to $Ag_{10}Br_{11}$ negative kink for comparison to the properties of Ag_2 adsorbed to an $Ag_{11}Br_{10}$ positive kink in order to compare the properties of these centers. We computed the equilibrium structures for these clusters. For Ag_3^+ at the negative kink, we found three different local energy minima depending upon the starting structure. These optimized structures include a linear geometry and two triangular geometries with different orientation with respect to the negative kink that is shown in Figure 5. The comparison of properties of the various centers given in Tables 2 and 7 shows that the Ag_2 center at the positive kink has an electron trap depth varying from 0.21 to 0.50 eV, while only one of the Ag_3^+ centers can trap electrons. This is not a deep trap. The relative energies of the different Ag_3^+ structures are rather similar, indicating the possibility of forming a distribution of clusters.

These results call attention to the fact that the properties of small silver clusters depend on their structure and hence mode of formation. They are most consistent with photolytic clusters forming at positive kinks. On the other hand, chemically formed clusters are expected to form on more predominant surface defects such as the negative kink or double kink. The present results show that if Ag_2 forms at a negative kink and then attracts a silver ion, the resulting center will have properties different than photolytic centers. This Ag_3^+ structure may or may not be able to trap electrons depending upon its structure. The Ag_2 center at a positive kink is a much deeper trap for electrons. These results for Ag_3^+ clusters could be interpreted to be consistent with microwave photoconductivity experiments of Tani,[23−25] indicating an electron trap nature for some chemically produced silver centers. They also point to the complexity of chemically formed centers since they may possess a range of geometries and properties depending upon the sites where they adsorb.

We can use the binding energy values in Tables 4 and 7 to evaluate whether the reaction

$$Ag^+ + Ag_2(-K) \rightarrow Ag_3^+(-K) \qquad (6)$$

is energetically favored. Using the binding energy of Ag^+ at a negative kink (4.72 eV), we find that the reaction is exothermic by −1.26, −1.30, or −0.56 eV for the three configurations of Ag_3^+ shown in Figure 5. Thus, there is no energetic barrier to adsorption of a silver ion at the silver dimer located at the negative kink. If an Ag_2 center forms by chemical treatment, it could be converted to Ag_3^+. However, we note from the data in Table 4, the only other defect site that would permit this reaction to be exothermic is the −DK site.

Substitutional Sulfide within a Positive Kink. Since positive kinks have been identified as favorable sites for formation and growth of silver clusters, we consider the effects of incorporation of substitutional sulfide ion. This process might be envisioned to happen during growth on the surface of AgBr when molecules of Ag_2S are present. We construct the $Ag_{11}Br_8S$ model shown in Figure 6, where S^{2-} replaces a Br^- ion right in the center of the positive kink and requires a nearest neighbor interstitial ion for compensation. We were interested in learning whether a significant relaxation takes place at such a site to stabilize a trapped electron such as that interpreted in photoconductivity experiments[3] and proposed in the Hamilton model of strong lattice coupling.[37] The cluster model was first relaxed with the earlier procedure where Born−Mayer terms were added between quantum mechanical ions and adjacent point ions. Then an electron was added and the change in energy determined upon relaxing from the neutral state geometry to equilibrium was calculated. The relaxation energy amounted to 0.24 eV and represents a kind of self-trapping induced by the electron. This relaxation involves displacements of the interstitial silver ion as a major component and is reflective of the electron coupling to the lattice. The electron affinity of a silver atom adsorbed to this model is calculated to be 4.56 eV and is sufficient to trap a second electron. When this electron is trapped, its excess energy must be dissipated and the nearby interstitial silver ion provides an excellent coupling to achieve this end. The resulting stabilized silver anion can attract a mobile silver interstitial ion and become converted to the stable Ag_2. The electron affinity of this and subsequent clusters are all greater than 3.6 eV and thus sufficient to trap electrons at the positive kink.

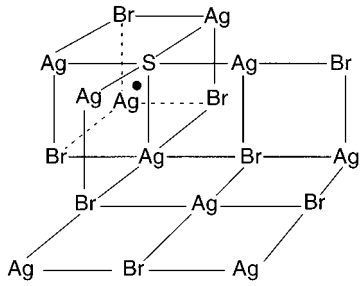

Figure 6. Drawing of the positive kink model containing a sulfide ion and a compensating silver ion denoted by the filled circle. The quantum cluster is embedded in the point ion arrays described in the text.

IV. Discussion

Detailed ab initio calculations of the gas-phase properties of silver clusters have been presented by several authors.[28,42−47] These methods have included configuration interaction and density functional treatments in order to include correlation energy effects. Interestingly, the different methods agree that the structure of small neutral silver clusters up to and including five atoms in size remains planar rather than three-dimensional compact structures. Thus, the favored structure of the tetramer is a rhombus and for the pentamer is a trapezoidal structure. In addition, the most stable structure of Ag_4^+ was shown to be a rhombus.[28] The results of our calculations for the tetramer on the silver bromide surfaces are somewhat similar to these gas-phase results in giving near planar structures and in the overall shape of a Ag_4 rhombus as most stable. Interestingly, detailed studies of the silver clusters with classical models showed[46,47] the need for three-, four-, and five-body forces in order to achieve the planar structure for the small silver clusters.

Attempts[48] have been made to compare two-body classical potential descriptions of silver clusters to the quantum mechanical gas-phase calculation of Bonacic-Koutecky et al.[28] The

classical calculations are based upon van der Waals interactions and charged induced dipole interaction terms and predict the most stable structure to be compact three-dimensional shapes in contrast to the results just mentioned with quantum mechanical methods. The analysis attempted to determine whether the energetics of small clusters allowed silver ion addition to the neutral cluster by a reaction

$$Ag^+ + Ag_{n-1} \rightarrow Ag_n^+ \quad (7)$$

The ab initio results of ref 28 give −1.64, −2.93, and −3.22 eV for $n = 2, 3, 4$, respectively, in the gas phase. We may use these values to approximately calculate the energy change for surface reaction by employing the calculated binding energy of an interstitial ion of 4.31 eV. Using this reference gives, +2.67, +0.99, and +0.96 eV for $n = 2, 3, 4$, respectively, for the surface reaction. Of course, for a surface reaction the polarization energy contribution needs to be considered. In the case of reaction 7, there is a unit positive charge on each side of the equation that to a first approximation cancels the polarization energy differences. Thus, with this approximation, we can compare to our calculations in Table 5 where the corresponding values at the positive kink are as follows: +1.89, +1.84, and +1.02 eV, for $n = 2, 3, 4$, respectively. There is broad agreement between the two sets of calculations that silver ions are more stable at interstitial sites than bound to neutral small silver clusters on the surface of AgBr. If we had used the binding energy of a silver ion to a negative kink (4.72 eV) as the reference state, the energetics calculated for these reactions would have been even more endothermic. Examining the present data for binding energies in Table 5 shows that reaction 7 is endothermic at the flat surface and also for most cluster sizes at the positive double kink. Cationic clusters that may exist at negatively charged kink sites are electrostatically equivalent to a neutral cluster at the positive kink. Thus, the results of both these ab initio calculations for silver clusters on surfaces and ab initio calculations in the gas phase corrected for surface adsorption are consistent with one another in predicting instability of small cationic silver clusters on the surface of AgBr and in disagreement with the classical two-body calculations used for analysis of photographic mechanisms in ref 48. The present analysis answers one of the questions posed in the Introduction that cationic clusters would not be expected to form in the photolytic mechanism.

We consider the mechanism of photolysis of AgBr starting at the unstable silver atom. Our calculations show that this atom has a deep electron trapping level on the order of 1 eV. Thus, during the atom lifetime an electron may be expected to diffuse to the center forming an anion, which can be further neutralized by an interstitial silver ion. The energy change for this reaction

$$Ag- + Ag^+_i \rightarrow Ag_2 \quad (8)$$

is calculated to be −0.3 eV as determined using a Born−Harber cycle using our calculated data as well as experimental constants. Thus, the silver atom presents a center that can trap electrons, followed by attraction of a silver ion to grow to the stable dimer state. This result resolves one of the questions posed in the Introduction and shows that the silver atom can indeed grow to the dimer stage and does not represent a wasted step from the standpoint of photoefficiency.

We turn to the question of the extent of the effect of surface site on the properties of the small silver clusters. The positive kink possesses a partial positive charge, and this promotes electron trapping into the valence levels of the neutral clusters. At the dimer, trimer, and tetramer this trap depth is calculated to be in the range of 0.2−0.5 eV, as indicated by the data in Table 2 for the different possible orientations of the neutral clusters at the site. Thus, electron trapping is possible at this site for all of these clusters. This behavior is different at the double kink, flat, and negative kink sites. In those sites, electrons cannot be trapped, and if a neutral cluster were formed, it would be susceptible to reaction with photoholes. Carrier trapping into the localized valence levels of silver clusters is strongly influenced by the electrostatic potential at the particular defect site. This behavior contrasts with shallow electron trapping due to Coulomb states caused by the bare kink site. In the latter case there is no valence level to accept the electron, and instead the electron is held in a diffuse state described by the effective mass approximation. For a unit charge this state has a mean radius of 23.9 Å in AgBr.[10] Thus the trapped electron is screened from the local site charge by the static dielectric constant. In contrast, the tightly held electrons in the silver cluster are barely screened.

We find support for the proposal of Tani that an Ag_3^+ center at a negative kink could trap electrons. If the center is formed first as Ag_2 by chemical reduction and then attracts a silver ion, it leads to a local structure that can be different than a dimer at the positive kink. The Ag_3^+ center has properties that depend strongly upon its structure with at least one form having favorable electron trapping properties. This type of center does not appear to be as deep a trap for electrons as the dimer at the positive kink, and it is not clear whether the cluster could grow to larger sizes.

Experiments[21−23] have indicated that chemically produced silver dimers are of two types. At smaller amounts of reducing agent, they trap holes and then electron trapping centers are formed at greater levels of reducing agent. While many details of the overall mechanism are unknown, a possible explanation of this result may be offered on the basis of these calculations. The composition of a silver bromide surface is predominately double kinks versus single kinks. Atomistic calculations[41] of silver bromide surfaces show that the double kink can form 0.30 eV more easily than the single kink. An estimate of the ratio of these sites based upon a Boltzmann factor gives 10^5 at room temperature. Thus, at low levels of reducing agent the silver dimers have a much greater chance of forming at double kinks, where the calculations indicate they would trap holes, but not electrons. The binding energy of the dimer to the double kink is large enough so that once formed there it would not easily diffuse away. At higher levels of reducing agent, more dimers will be formed and the chances of forming at a single kink become greater. The calculations indicate that these dimers would trap electrons.

We examined a model for sulfur sensitization where the sulfur becomes incorporated into a positive kink site. This site might be envisioned to form through diffusion of Ag_2S molecules to a kink site and partial growth with silver and halide ions to lead to a kink site. The center requires charge compensation by a silver ion since the sulfide replaces a bromide ion in the lattice. The most stable site calculated for the interstitial silver ion is in the cell containing the sulfide ion as shown in Figure 6. This site provides an electron trapping site which becomes deepened by relaxation of the interstitial silver ion and the neighboring crystal ions by the presence of the electron. Our calculations predict a relaxation energy of 0.24 eV and this value is close to the range of 0.3−0.4 eV that experiments[49−51] have reported for the electron trap depth at sulfide. Our calculations are only expected to provide a qualitative guide to this energy since the

cluster size limits the number of lattice ions that can be allowed to relax. It should be emphasized that many factors beyond the energy are involved in sensitization so that a specific active site is not proposed in this work.

It should be recalled that even as detailed a calculation as we report here is an approximation to the complex photographic system. A grain of AgBr contains sensitizing dyes and gelatin on the surface, and the interior contains a space charge layer. The present model is that of a bare surface and one where the electronic energy bands are flat. In light of these uncertainties, vibrational effects due to temperature were not included into any model considerations. In the photographic system ambient gases such as O_2 can possibly play a role in the steps involving an electron and leading to silver cluster formation. These possible steps were not considered in this study. Thus, the results presented here should be viewed as a somewhat idealized system where the conditions are well-defined, but they could be somewhat different than a particular photographic system.

Appendix

We have examined the point-ion approximation used to simulate the Madelung field surrounding the embedded cluster representing AgBr and containing various sites for silver cluster adsorption. Some classifications such as the Phillips ionicity scale[52] place the AgBr ionicity at 0.85 rather than the full ionicity of 1.0. We tested the use of different charge values within the point charge array to understand whether this effect would be significant in our calculation. We employed a model for the positive kink $(AgBr)_4$ using basis sets employed in earlier work.[7] We studied the properties of adsorbed Ag and Ag_2 at the positive kink using fractional rather than full ionic charges for the point ion array. Table A1 shows the calculated IP and EA values. We observe that the effects of the charge values are small over the range we have considered that extends well beyond values reasonable for the AgBr ionicity. Thus, the point charge approximation appears justified for use in application to AgBr.

We observe displacements of the silver and bromide ions from their ideal positions dureing the second stage of the calculation described in Methods. The displacements are small, but not negligible. We show typical values for Ag2 adsorbed at a positive kink in Table A2.

TABLE A1: Calculated Values of IP and EA without Polarization Energy Correction for Ag, Ag_2 Adsorption at the Positive Kink $(AgBr)_4$ Model Using Different Fraction Charges[a]

cluster	property	charge = ± 1.0	charge = ± 0.85	charge = ± 0.70
Ag	IP	8.69	8.51	8.56
Ag	EA	4.45	4.31	4.43
Ag_2	IP	8.92	8.68	8.69
Ag_2	EA	3.92	3.77	3.87

[a] No lattice polarization energy corrections are applied.

TABLE A2: Unrelaxed Positions[a] and Displacement of AgBr Ions at a Positive Kink upon Relaxation

	unrelaxed positions			displacements		
ion	*X*	*Y*	*Z*	*X*	*Y*	*Z*
Ag	1.0	0.0	0.0	0.10	0.01	0.01
Br	1.0	1.0	0.0	0.07	0.04	0.06
Ag	0.0	1.0	0.0	0.01	0.00	0.01
Br	1.0	1.0	0.0	0.05	0.03	0.09
Ag	2.0	1.0	0.0	0.05	0.04	0.03

[a] Units of nearest-neighbor distance.

References and Notes

(1) Brady, L. E.; Hamilton, J. F. *J. Appl. Phys.* **1966**, *37*, 2268.

(2) Eachus, R. S.; Olm, M. T.; Janes, R.; Symons, M. R. C. *Phys. Status Solidi B* **1989,** *152*, 583.

(3) (a) Deri, R. J.; Spoonhower, J. P.; Hamilton, J. F. *J. Appl. Phys.* **1985,** *57*, 1968. (b) Deri, R. J.; Spoonhower, J. P. *J. Appl. Phys.* **1985**, *57*, 2806.

(4) Eachus, R. S.; Marchetti, A. P.; Muenter, A. A. *Annu. Rev. Phys. Chem.* **1999,** *50*, 117.

(5) (a) James, T. H. In *The Theory of the Photographic Process*, 4th ed.; Mcmillan: New York, 1977. (b) Tani, T. *Photographic Sensitivity*; Oxford University Press: New York, 1995.

(6) (a) Hamilton, J. F.; Logel, P. C. *Photogr. Sci. Eng.* **1974**, *18*, 507. (b) Fayet, P.; Granzer, F.; Hegenbart, G.; Moisar, E.; Pischel, B.; Woste, L. *Phys. Rev. Lett.* **1985**, *55*, 3002.

(7) (a) Baetzold, R. C. *Photogr. Sci. Eng.* **1975**, *19*, 11. (b) Baetzold, R. C. *J. Phys. Chem. B* **1997**, *101*, 8180.

(8) Hamilton, J. F.; Baetzold, R. C. *Photogr. Sci. Eng.* **1981**, *25*, 189.

(9) (a) Gurney, R. W.; Mott, N. F. *Proc. R. Soc. London* **1938**, *A164*, 151. (b) Mott, N. F.; Gurney, R. W. *Electronic Processes in Ionic Crystals*; Clarendon: Oxford, U.K., 1948.

(10) Hamilton, J. F. *Adv. Phys.* **1988**, *37*, 359.

(11) Hailstone, R. K. *J. Phys. Chem.* **1995**, *B99*, 4414.

(12) Mitchell, J. W. *J. Imaging Sci. Technol.* **1995**, *39*, 193.

(13) Webb, J. H. *J. Opt. Soc. Am.* **1933**, *23*, 157.

(14) Spencer, H. E.; Brady, L. E.; Hamilton, J. F. *J. Opt. Soc. Am.* **1967**, *57*, 1020.

(15) Spencer, H. E. *Photogr. Sci. Eng.* **1967**, *11*, 352.

(16) Spencer, H. E. *J. Photogr. Sci.* **1972**, *20*, 143.

(17) Moisar, E.; Granzer, F.; Dantrich, D.; Palm, E. *J. Photogr. Sci.* **1977**, *25*, 12.

(18) Moisar, E.; Granzer, F.; Dantrich, D.; Palm, E. *J. Photogr. Sci.* **1980**, *28*, 71.

(19) Tani, T. *Photogr. Sci. Eng.* **1971**, *15*, 28.

(20) Tani, T. *Photogr. Sci. Eng.* **1971**, *15*, 181.

(21) Tani, T.; Murofushi, M. *J. Imaging Sci. Technol.* **1994**, *38*, 1.

(22) Guo, S.; Hailstone, R. K. *J. Imaging Sci. Technol.* **1996**, *40*, 210.

(23) Tani, T. *J. Imaging Sci. Technol.* **1997**, *41*, 577.

(24) Tani, T. J. *J. Imaging Sci. Technol.* **1998**, *42*, 577.

(25) Tani, T.; Tasaka, T.; Murofushi, M.; Hosoi, K.; Hirano, A. *J. Imaging Sci. Technol.* **1999**, *47*, 1.

(26) Oku, Y.; Kawasaki, M. *J. Phys. Chem. B* **1998**, *102*, 9061.

(27) Marchetti, A. P.; Muenter, A. A.; Baetzold, R. C.; McCleary, R. T. *J. Phys. Chem. B* **1998**, *102*, 5287.

(28) Bonacic-Koutecky, V.; Cespiva, L.; Fantucci, P.; Koutecky, J. *J. Chem. Phys.* **1993**, *98*, 7981.

(29) (a) Becke, A. D. *Phys. Rev.* **1988**, *A33*, 3098. (b) Lee, C.; Wang, W.; Parr, R. G. *Phys. Rev.* **1988**, *B37*, 785. (c) Johnson, B. G.; Gill, P. M.; Pople, J. A. *J. Chem. Phys.* **1993**, *98*, 5612.

(30) Frisch, M. J.; Trucks, G. W.; Schlegel, H. B.; Scuseria, G. E.; Robb, M. A.; Cheesman, J. R.; Zakrzewski, V. G.; Montgomery, J. A.; Stratmann, R. E.; Burant, J. C.; Dapprich, S.; Millam, J. M.; Daniels, A. D.; Kudin, K. N.; Strain, M. C.; Farkas, O.; Tomasi, J.; Barone, V.; Cossi, M.; Cammi, R.; Mennucci, B.; Pomelli, C.; Adamo, C.; Clifford, S.; Ochterski, J.; Petersson, G. A.; Ayala, P. Y.; Cui, Q.; Morakuma, K.; Malick, D. K.; Rabuck, A. D.; Raghavachari, K.; Foresman, J. B.; Cioslowski, J.; Ortiz, J. V.; Stefanov, B. B.; Lui, G.; Liashenko, A.; Piskorz, P.; Komaromi, I.; Gomperts, R.; Martin, R. L.; Fox, D. J.; Keith, T.; Al-Laham, M. A.; Peng, C. Y.; Nanayakkara, A.; Gonzalez, C.; Challacombe, M.; Gill, P. M. W.; Johnson, B. G.; Chen, W.; Wong, M. W. Andres, J. L.; Head-Gordon, M.; Replogle, E. S.; Pople, J. A. *Gaussian 98* (Revision A.7); Gaussian, Inc.: Pittsburgh, PA, 1998.

(31) Tasker, P. W. *Philos. Mag.* **1979**, *39*, 19.

(32) Catlow, C. R. A.; Corish, J.; Harding, J. H.; Jacobs, P. W. M. *Philos. Mag.* **1987**, *A55*, 481.

(33) Sushko, P. V.; Shluger, A. L.; Catlow, C. R. A. *Surf. Sci.* **2000**, 450, 153.

(34) Sushko, P. V.; Shluger, A. L.; Baetzold, R. C.; Catlow, C. R. A. *J. Phys. C: Condens. Matter* **2000**, *12*, 8257.

(35) (a) Hay, P. J.; Wadt, W. R. *J. Chem. Phys.* **1985**, *82*, 270. (b) Wadt, W. R.; Hay, P. J. *J. Chem. Phys.* **1985**, *82*, 284. (c) Hay, P. J.; Wadt, W. R. *J. Chem. Phys.* **1985**, *82*, 299.

(36) (a) Victora, R. H. *Phys. Rev.* **1997**, *B56*, 4417. (b) Kunz, A. B. *Phys. Rev.* **1982**, *B26*, 2070.

(37) Ehlers, A. W.; Bohme, M.; Dapprich, S.; Goffi, A.; Hollwarth, A.; Jonas, V.; Kohler, K. F.; Stegmann, R.; Veldkamp, A.; Frenking, G. *Chem. Phys. Lett.* **1993**, *208*, 111.

(38) Brown, F. C. *The Physics of Solids*; Benjamin: New York, 1967.

(39) Hamilton, J. F. *J. Imaging Sci.* **1990**, *34*, 1.

(40) Baetzold, R. C.; Hamilton, J. F. *Surf. Sci.* **1987**, *179*, L85.

(41) Baetzold, R. C. *Phys. Rev.* **1995**, *B52*, 11424.

(42) Balasubramanan, K. *J. Mol. Struct. (THEOCHEM)* **1989**, *202*, 291.
(43) Bauschlicher, C. W., Jr.; Langhoff, S. R.; Partridge, H. *J. Chem. Phys.* **1990**, *93*, 8133.
(44) Santamaria, R.; Kaplan, I. G.; Novaro, O. *Chem. Phys. Lett.* **1994**, *218*, 395.
(45) Poteau, R.; Heully, J.-L.; Spagelman, F. *Z. Phys. D* **1977**, *40*, 479.
(46) Garzon, I. L.; Kaplan, I. G.; Santamaria, R.; Novaro, O. *J. Chem. Phys*. **1998**, *109*, 2176.
(47) Kaplan, I. G.; Santamaria, R.; Novaro, O. *Mol. Phys*. **1995**, *84*, 105.
(48) (a) Mitchell, J. W. *J. Photogr. Sci*. **1996**, *44*, 82. (b) Mitchell, J. W. *Photogr. Sci. Eng.* **1978**, *22*, 1. (c) Mitchell, J. W. *Photogr. Sci. Eng.* **1979**, *23*, 1.
(49) Kanzaki, H.; Tadakuma, Y. *J. Phys. Chem. Sol.* **1997**, *58*, 221; **1994**, *55*, 631.
(50) Kellogg, L. M. *Photogr. Sci. Eng.* **1974**, *18*, 378.
(51) Hamilton, J. F.; Harbison, J. M.; Jeanmaire, D. L. *J. Imaging Sci.* **1988**, *32*, 17.
(52) Phillips, J. C. *Bonds and Bands in Semiconductors*; Academic Press: New York, 1973.